

NO Inhibitory, Farnesoid X Receptor, and Cytotoxic Activities of Phytochemical Composition Isolated from *Aglaia perviridis*

Donghua Cao^{1*}, Binyuan Jiang¹, Linghui Cao¹, Manli Jiang¹

and Xueting Liu¹

The Affiliated Changsha Central Hospital, Hengyang Medical School, University of South China,
Changsha 410004, P. R. China

(Received April 11, 2023; Revised May 24, 2023; Accepted May 29, 2023)

Abstract: To search for novel and bioactive agents from the genus *Aglaia*, phytochemical investigation on the leaves and twigs of *A. perviridis* was performed, leading to the isolation of twenty-six compounds. Their structure was determined mainly by the NMR, ESI-MS spectra data, and by comparison with previously described compounds. Compounds **6–8**, **11–13**, **16**, **18–20**, and **22–26** were firstly reported from *A. perviridis*. Besides, the NO inhibitory, Farnesoid X receptor, and cytotoxic activities of selected compounds were firstly evaluated. 1 α H,5 α H-guaia-6-ene-4 β ,10 β -diol (**7**), 2'-hydroxy-4,4',6'-trimethoxychalcone (**22**), and 3-hydroxy-5,7,4'-trimethoxyflavone (**23**) showed moderate nitric oxide inhibitory activity with IC₅₀ values of 27.44 \pm 1.70, 22.29 \pm 1.53, and 19.29 \pm 3.96 μ M, respectively; piscidinol A (**11**) and hispidol B (**12**) firstly showed moderate agonistic activities on Farnesoid X receptor with the EC₅₀ values of 6.19 \pm 1.08 and 8.61 \pm 0.32 μ M, respectively; Among these compounds, lochmolin F (**6**) exhibited the strongest cytotoxic effect on SiHa cells with the IC₅₀ value of 19.58 \pm 0.21 μ M. Further flow cytometry and western blot analysis demonstrated that lochmolin F (**6**) could induce cell apoptosis and S cell cycle arrest in the SiHa cells. These results first emphasized the potential of lochmolin F (**6**) as lead compound for developing anti-cancer drugs.

Keywords: *Aglaia perviridis*; phytochemical composition; anti-inflammatory; FXR; cytotoxic activities. © 2023 ACG Publications. All rights reserved.

1. Introduction

The genus *Aglaia* is the largest genus of the angiosperm plant family Meliaceae, which comprises more than 120 species that are mainly distributed in the tropical and sub-tropical rainforest areas of

* Corresponding author: E-Mail: caodonghua14@mails.ucas.ac.cn Phone:086-188-13107708

Phytochemical composition isolated from *Aglaia perviridis*

Southeast Asia and the Pacific region [1], of which seven species and one variant grow in China [2]. Some *Aglaia* species have been traditionally used as folk medicines in China for treating fever, cough, diarrhoea, and contused wounds [3]. To date, various amides, triterpenoids (e.g., cycloartanes, dammaranes, and tirucallanes), and flavaglines (e.g., cyclopenta[b]benzofurans, cyclopenta[bc]benzopyrans, and benzo[b]oxepines) have been isolated from this genus [4-9]. In particular, some of the flavagline derivatives showing interesting antiviral [10, 11], antifungal [12], antineoplastic [13], cytotoxic [14, 15], and insecticidal [16, 17] activities have been found. Potential anti-inflammatory activity was also observed for some triterpenes [18, 19]. In continuation of the discovery of novel and bioactive natural products from plants of *Aglaia* species, the chemical constituents of the species *A. perviridis*, a wild shrub indigenous to Yunnan Province of China were investigated. Their structure was determined mainly by the NMR, ESI-MS spectra data, and by comparison with previously described compounds. Selected isolated compounds were firstly evaluated for their Nitric oxide (NO) inhibitory, Farnesoid X receptor (FXR), and cytotoxic activities against four cancer lines (the A549, SiHa, 5-8F, and HepG2 cell lines). In addition, the action mechanism of lochmolin F (**6**) inhibiting SiHa cell proliferation was further studied. Herein, we report the isolation, structural elucidation, and activity evaluation of selected the isolates.

2. Materials and Methods

2.1. Chemicals and Reagents

The NMR spectra were obtained on Bruker Avance DRX500 and Bruker Avance III HD 600 spectrometer (Bruker corporation, Karlsruhe, German), using tetramethylsilane as an internal standard. ESIMS were carried out on a Shimadzu UPLC-IT-TOF mass spectrometer (Shimadzu Corporation, Japan). Semi-preparative HPLC was performed on a Waters 600 pump system with a 2996 photodiode array detector by using a YMC-Pack ODS-A column (300 × 10 mm, S-5 μm). Column chromatography was run over silica gel (200–300 mesh, Qingdao Marine Chemical Factory, Qingdao, China). Sephadex LH-20 gel (40–70 μm, Amersham Pharmacia Biotech AB, Uppsala, Sweden). Spots were detected firstly on TLC (Qingdao Marine Chemical Factory) under 254 nm UV light and then by spraying with 10% H₂SO₄ in ethanol for plate heating. All solvents used were of analytical grade (Shanghai Chemical Reagents Co. Ltd), and all solvents used for HPLC were of chromatographic grade (J & K Scientific Ltd.). 3-(4,5-dimethylthiazol-2-yl)-5-(3-carboxymethoxy-phenyl)-2-(4-sulfophenyl)-2H-tetrazolium (MTS) was purchased from Promega Corporation (Madison, Wisconsin, USA). Annexin V-FITC apoptosis detection kit was purchased from Yeasen Biotechnology (Shanghai) Co., Ltd. Antibodies against cyclin A2, CDK2, cyclin D1, and GAPDH were purchased from Cell Signaling Technology (Beverly, MA, USA) (all used at 1:1000 dilutions). Griess Reagent was purchased from Promega Corporation (Madison, Wisconsin, USA). Hoechst 33342 was purchased from Beyotime Biotechnology (Shanghai).

2.2. Plant Material

The twigs and leaves of *A. perviridis* were collected from Menglun town (101°25'E, 21°41'N), Mengla Country, Yunnan Province, People's Republic of China at an altitude of 570 m in May 2016, and they were

identified by Professor Youkai Xu from Xishuangbanna Tropical Botanical Garden, Chinese Academy of Sciences (XTBG). A voucher specimen (HITBC-028497) is deposited in the herbarium at XTBG.

2.3. Plant Extraction

The air-dried powdered twigs and leaves (5 kg) of *A. perviridis* were extracted with 95% EtOH (3×30 L, 7 days each time) at room temperature. After evaporation of the solvent under reduced pressure, the residue (365 g) was suspended in H₂O (1 L) and partitioned successively with petroleum ether (3 × 1.0 L) and EtOAc (3 × 1.0 L). The petroleum ether extract (112 g) was subjected to silica gel column chromatography (CC) eluted with CHCl₃/MeOH (50:1-1:1, v/v) to afford four fractions (P-1–P-4). Fraction P-1 (20 g) was repeatedly subjected to silica gel CC eluted with CHCl₃/Me₂CO (50:1–2:1, v/v), to yield **9** (8 mg) and **10** (15 mg). Fraction P-3 (15 g) was separated by Sephadex LH-20 gel CC eluted with MeOH/H₂O gradient (1:1–4:1, v/v) to afford subfractions P-3a–P-3d. Fraction P-3a (3 g) was purified by semipreparative HPLC (MeCN/H₂O, 70:30, v/v, 3 mL/min) to yield **11** (9 mg), **12** (24 mg), and **13** (60 mg). Fraction P-3b (3 g) was purified by semipreparative HPLC (MeCN/H₂O, 52:48, v/v, 3 mL/min) to yield **6** (4 mg), **7** (6 mg), and **8** (3 mg). Fraction P-3d (4 g) was further purified by semipreparative HPLC (MeCN/H₂O, 60:40, v/v, 3 mL/min) to yield **1** (16 mg), **2** (5 mg), **3** (5 mg), **4** (4 mg), and **5** (5 mg). The ethyl acetate extract (105 g) was chromatographed over a microporous resin, eluted with gradient mixtures of MeOH/H₂O (20:80, 40:60, 60:40, 80:20, and 100:0, v/v) to afford five major fractions (E-1–E-5). Fraction E-3 (60 g) was separated by silica gel CC eluted with CHCl₃/MeOH (50:1–1:1, v/v) to yield three major fractions E-3a–E-3c (11.0, 7.2, and 8.0 g, respectively). Fraction E-3a (11.0 g) was first chromatographed on a Sephadex LH-20 gel column eluted with MeOH and then purified with semipreparative HPLC (MeCN:H₂O, 69:31, 3 mL/min) to yield **14** (7 mg), **15** (9 mg), **19** (12 mg), and **20** (4 mg). Fraction E-3c (8.0 g) was separated by silica gel CC eluted with CHCl₃/EtOAc (20:1–1:1, v/v), followed by Sephadex LH-20 gel purification eluted with MeOH, to afford **16** (3 mg), **17** (4 mg), and **18** (4 mg). Fraction E-4 (35 g) was subjected to silica gel CC, to yield two subfractions E-4a–E-4b. Fraction E-4a (2.0 g) was purified by semipreparative HPLC (MeCN/H₂O, 60:40, v/v, 3 mL/min) to afford **21** (4 mg), **22** (12 mg), **23** (50 mg), and **24** (4 mg). Fraction E-4b (16.0 g) was purified by semipreparative HPLC (MeCN/H₂O, 55:45, v/v, 3 mL/min) to afford **25** (3 mg), **26** (3 mg), respectively. All of the compounds met the criteria of $\geq 95\%$ purity, as determined by NMR analysis.

2.4. Cell Culture

A549 (lung carcinoma), SiHa (cervical carcinoma), 5-8F (nasopharyngeal carcinoma), HepG2 (hepatocellular carcinoma), and HUVEC (human cervical epithelial cells) cells were purchased from American Type Culture Collection (ATCC, Manassas, VA, USA). The RAW264.7 macrophages were obtained from Kunming Institute of Zoology, Chinese Academy of Sciences). All cells were cultured in DMEM medium supplemented with 10% FBS, containing 100 units/mL penicillin and 100 µg/mL streptomycin (1% PS) at 37 °C in the presence of 5% CO₂.

2.5. Assay for Inhibition Ability toward LPS-induced NO Production and Cytotoxicity Testing

The RAW264.7 macrophages were seeded in 96-well plates with 1×10^4 cells/well and allowed to adhere for 12 h at 37 °C in a humidified atmosphere containing 5% CO₂. Then, the RAW264.7 macrophages were treated with tested compounds and 1 µg/mL lipopolysaccharide (LPS) for 24 h. NG-monomethyl L-arginine (Sigma) was used as a positive control. An equal volume of DMSO was used as vehicle control. The cell viability was determined by MTS assay before NO production assay, and the NO production was measured by the accumulation of nitrite in the culture supernatants using the Griess Reagent System at OD 550 as previously reported [20].

2.6. Cell Viability Assay

The obtained compounds were tested for their cytotoxic activity against the A549, SiHa, HUCEC, 5-8F, and HepG2 cancer cell lines using the MTS method. Briefly, 100 µL adherent cells were seeded into each well (5×10^3 cells/well) of 96-well cell culture plates and allowed to adhere for 18 h before testing drug addiction. Each tumor cell line was exposed to a test compound at concentrations of 0, 2.5, 5, 10, 20, and 40 µM in DMSO in triplicate for 24 h or 48 h, with cisplatin as the positive control. An equal volume of DMSO was used as vehicle control. After 24 h or 48 h incubation, the medium was removed. Subsequently, 100 µL medium and 20 µL MTS solution was added to each well, which was incubated for another 4 h to give a formazan product. The OD value of each well was measured at 490 nm using a Biorad 680 instrument.

2.7. Cell Cycle Analysis

For analyzing the cell cycle distribution, flow cytometry was performed as described previously [21]. In brief, SiHa cells (4×10^5 cells/well) were plated at 6-well plates and challenged on compounds for 24 h and 48 h, respectively. Next, the cells were collected, washed twice with cold PBS, and fixed in 70% cold ethanol at 4 °C overnight. After being washed with chilled PBS, the cells were incubated with RNase A (0.5 mg/mL) at 37 °C for 1 h and then stained with PI (final concentration of 10 µg/mL) at room temperature in the dark for 15 min. Afterward, the cell cycle analysis was carried out on a flow cytometer (FACS Calibur, BD Biosciences, San Jose, USA).

2.8. Apoptosis Detection

SiHa cells were seeded in 12-well plates at a density of 2×10^5 cells/well and incubated with compounds for 24 h and 48 h, respectively. After treatment, the cells were harvested and stained with the Annexin V-FITC apoptosis detection kit according to the manufacturer's instructions. Then, stained cells were analyzed by a flow cytometer.

2.9. FXR Coactivator Interaction Assay

The FXR coactivator interaction assay was performed in 384-well solid-bottom plates. A mixture of 5 nM purified, GST-tagged, human FXR LBD protein and 5 nM biotinylated coactivator steroid receptor coactivator-1 peptide (CPSSHSSLTERHKILHRLQLQEGSPS, Anaspec), 25 $\mu\text{g}/\text{mL}$ anti-GST acceptor (PerkinElmer), and streptavidin-conjugated AlphaScreen beads were added into the assay buffer containing 50 mM Tris (pH = 8.0), 50 mM KCl, 0.1% BSA, and 2 mM DTT with test compounds in dose-response. The plates were incubated for 2 h at room temperature and read on an Envision (PerkinElmer) at 570 nm. The model assessing fit is a sigmoidal dose-response (variable slope). Each compound is tested in three independent experiments with the EC_{50} value shown as mean \pm SD. Control assays are performed with obeticholic acid [22].

2.10. Statistical Analysis

All data were presented as mean \pm standard deviation. Three independent experiments were conducted for *in vitro* study. IC_{50} values (μM) from cell viability assay were calculated from dose-response curve-fitting *via* nonlinear regression analysis on GraphPad Prism 8.0 (GraphPad Software, San Diego, CA, USA). Significant differences between experimental and vehicle groups were evaluated with a one-way analysis of variance followed by Tukey's test. $p < 0.05$ or < 0.01 were considered statistically or highly statistically significant, respectively.

3. Results and Discussion

3.1. Isolation and Identification of Compounds

The 95% ethanol extract of the twigs and leaves of *A. perviridis* was subjected to silica gel column chromatography, Sephadex LH-20, and semi-preparative reversed-phase HPLC to obtain 26 secondary metabolites, pyramidatine (**1**) [23], perviridamide (**2**) [24], 4-hydroxy-pyramidatine (**3**) [24], silvestrol (**4**) [13], episilvestrol (**5**) [13], lochmolin F (**6**) [25], $1\alpha\text{H},5\alpha\text{H}$ -guaia-6-ene- $4\beta,10\beta$ -diol (**7**) [26], 15-hydroxy- α -cadinol (**8**) [27], cabraleahydroxylactone (**9**) [28], cabraleadiol (**10**) [29], piscidinol A (**11**) [30], hispidol B (**12**) [31], heteroclitalactone M (**13**) [32], $2\beta,2\beta$ -dihydroxy- 5α -pregn-17(20)-(Z)-en-16-one (**14**) [33], lansisterone E (**15**) [34], β -sitosterol 3-*O*- β -glucoside (**16**) [35], (+) eudesmin (**17**) [36], (–) eudesmin (**18**) [37], forsythenin (**19**) [38], epipinoresinol (**20**) [39], naringenin trimethyl ether (**21**) [40], 2'-hydroxy-4,4',6'-trimethoxychalcone (**22**) [41], 3-hydroxy-5,7,4'-trimethoxyflavone (**23**) [42], 5-hydroxy-7,4'-dimethoxyflavanone (**24**) [43], ethyl asterrate (**25**) [44], matairesinol (**26**) [45]. Their structures were elucidated by NMR, ESI-MS spectra data as well as comparison with those reported in the literature. Compounds **6–8**, **11–13**, **16**, **18–20**, and **22–26** were firstly reported from the species.

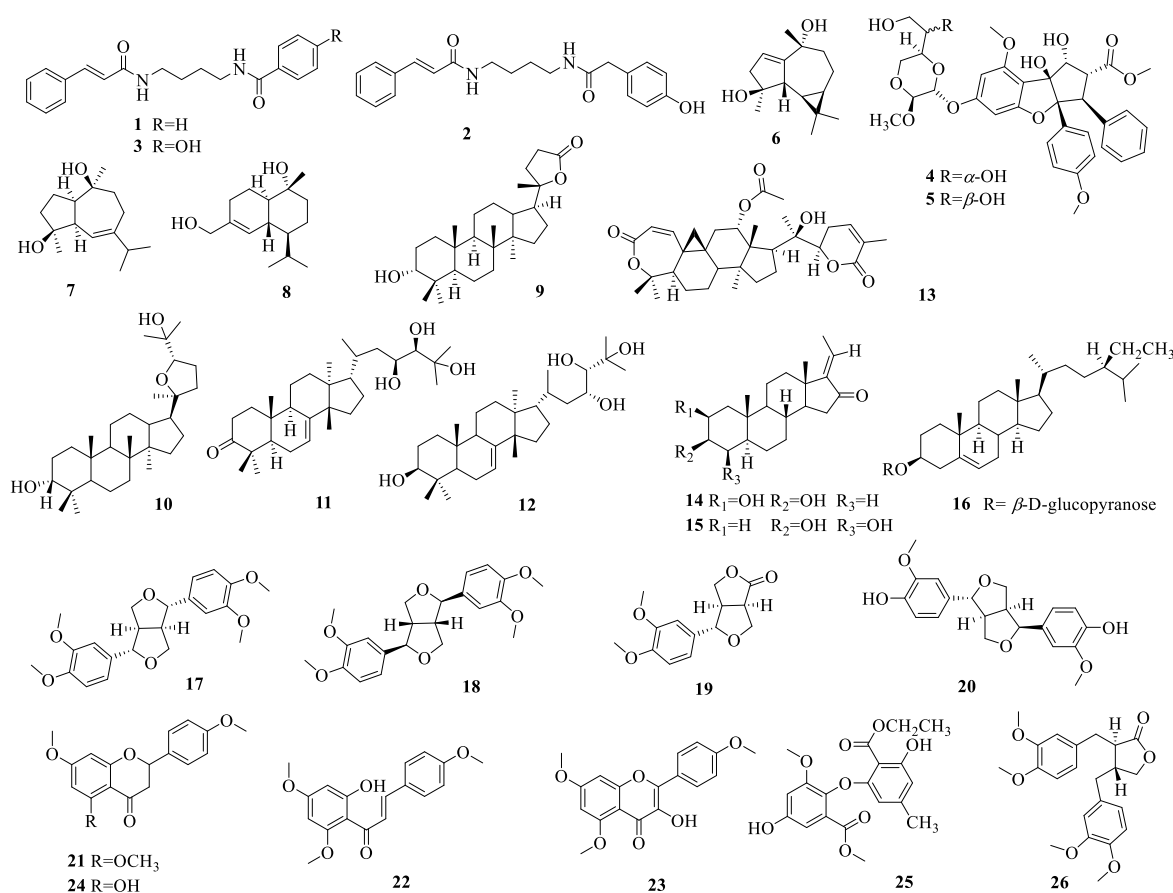
Phytochemical composition isolated from *Aglaia perviridis*

Figure 1. The structure of compounds 1–26

3.2. NO Inhibitory Activity of Compounds

To discover effective NO inhibitors, selected compounds were evaluated for their NO inhibitory activity on LPS-induced RAW264.7 cell lines. Firstly, the cell viability of selected compounds was determined by MTS method [46]. The results indicated that except compounds 1–6, 11, 12, and 14–16, other compounds do not effect on RAW264.7 cell viability at the concentration of 50 μ M, so they were further evaluated for their NO inhibitory activity in the LPS-induced RAW264.7 cell lines using a Griess Reagent System. Compounds 7, 22, and 23 showed moderate NO inhibitory activity with IC₅₀ values of 27.44 \pm 1.70, 22.29 \pm 1.53, and 19.29 \pm 3.96 μ M, respectively. Compounds 8, 13, and 21 exhibited weak NO inhibitory activity with IC₅₀ values of 37.96 \pm 1.58, 46.70 \pm 2.38, and 33.71 \pm 2.79 μ M, respectively (Table 1). Previous studies have reported that compound 7 exhibited cytotoxicities against the three human cancer cell lines H460, MCF-7, and PC-3 with IC₅₀ values of 56.7 \pm 1.4 μ M, 76.7 \pm 1.4 μ M, and 69.0 \pm 1.9 μ M, respectively [26]; compound 8 exhibited inhibitory effects on NO production of BV-2 microglia activated by LPS with IC₅₀ values of 19.89 \pm 0.83 μ M [47], which is consistent with the result in this study; compound 21 showed significant molluscicidal activity with LC₅₀ values of 3.9 μ g/mL [48]; compound 22 exhibited the strongest antioxidant properties with values of 42.23, 1497.22, and 781.53 mg TE/g against ABTS, CUPRAC, and FRAP assays, respectively [49], and antifungal activity [50], compound 23 were found to be strong DPPH free radical scavengers with IC₅₀ values of 119 μ M and showed strong inhibition activity towards EBV activation in Raji cells [51]. This study is the first to report the NO inhibitory activity

of these compounds, providing more candidate compounds for the development of anti-inflammatory drugs.

Table 1. Effect of selected compounds on LPS-induced NO production in RAW264.7 cells^a

Compound	IC ₅₀ /μM	Compound	IC ₅₀ /μM
7	27.44±1.70	19	N.T.
8	37.96±1.58	20	>50
9	>50	21	33.71±2.79
10	>50	22	22.29±1.53
13	46.70±2.38	23	19.29±3.96
17	>50	24	>50
18	>50	25	>50
NG-monomethyl L-arginine ^b	14.17±1.08	26	>50

^aData are represented as mean ± SEM (*n* = 3); N.T.: Not tested. ^b Positive controls.

3.3. FXR Activity Evaluations for selected Compounds

FXR plays a key role in bile acid homeostasis, inflammation, fibrosis, and metabolism of lipids and glucose and becomes a promising therapeutic target for nonalcoholic steatohepatitis (NASH) or other FXR-dependent diseases [22]. To discover novel FXR agonists, selected compounds were evaluated for their FXR bioactivity. The reported FXR agonist obeticholic acid was selected as the positive control. As shown in Table 2, the results indicated that compounds **11** and **12** showed moderate agonistic activities on FXR with the EC₅₀ value of 6.19±1.08 and 8.61±0.32 μM, respectively. Previous studies have mainly reported the antitumor activity of compounds **11** and **12** against various tested cancer cell lines, such as KB, MCF-7, KB-C2, P-388, RT112, HCT-116, and M231 [52-56]. They were triucallane-class triterpenoids, which structure was different from reported bile acid-derived FXR agonists that bring severe pruritus and an elevated risk of cardiovascular disease for patients [57, 58]. Thus, further structural modifications to compounds **11** and **12** were expected to develop a non-bile acid FXR agonist.

Table 2. The Agonistic Activities on Farnesoid X receptor of selected compounds^a

Compound	EC ₅₀ (μM)	Compound	EC ₅₀ (μM)
1	>20	13	N.T.
2-6	N.T.	14	>20
7	>20	15	>20
8	>20	16-24	N.T.
9	>20	25	>20
10	>20	26	N.T.
11	6.19±1.08	obeticholic acid ^b	0.32±0.01
12	8.61±0.32		

^aData are represented as mean ± SEM (*n* = 3); N.T.: Not tested. ^b Positive controls.

3.4. Evaluation of Cytotoxicity Activities of Selected Compounds

Except for compounds **4** and **5**, other compounds were evaluated for their cytotoxicity against four cancer cell lines (the A549, SiHa, 5-8F, and HepG2 cell lines) by the MTS method [46]. Only compounds **6** and **11** showed cytotoxicity against SiHa cell lines with the IC₅₀ value of 19.58±0.21 and 29.74±0.08 µM, respectively, and compounds **6** and **11** showed cytotoxicity against 5-8F cell lines with the IC₅₀ value of 26.51±0.42 and 20.89±0.16 µM, respectively (Table 3). Among these compounds, compound **6** exhibited the strongest cytotoxic effect on SiHa cells. To date, compound **6** has been reported to be isolated only from *Sinularia lochmodes* and has no cytotoxic activity against tumor cell lines HeLa, SK-Hep1 and B-16, as well as anti-inflammatory activity against the accumulation of pro-inflammatory iNOS and COX-2 proteins in RAW264.7 macrophage cells [25]. Piscidinol A (**11**) was reported to exhibit moderate cytotoxicity against various human cancer cell lines PC3, BGC-823, KE-97, KB, Huh-7, jurkat, and MCF-3 (IC₅₀ = 11.8, 67.5, 70.0, 35.4, 40.3, and 25.8 µM, respectively) [52, 53]. Thus, the action mechanism of compound **6** inhibiting SiHa cell proliferation was further studied.

Table 3. Cytotoxic activities of selected compounds against tumour cell lines (IC₅₀ µM)^a

Compound	A549	SiHa	5-8F	HepG2
1-3	>40	>40	>40	>40
4-5	N.T.	N.T.	N.T.	N.T.
6	>40	19.58±0.21	26.51±0.42	>40
7-10	>40	>40	>40	>40
11	>40	29.74±0.08	20.89±0.16	>40
12-26	>40	>40	>40	>40
Cisplatin ^b	8.5±0.22	22.31±0.03	3.0±0.43	12.52±0.18

^a Data are represented as mean ± SEM (*n* = 3); N.T.: Not tested. ^b Positive controls.

3.5. The Action Mechanism of Lochmolin F (**6**) Inhibiting SiHa Cell Proliferation

3.5.1. Lochmolin F (**6**) Inhibited Cell proliferation in SiHa Cell Lines

As shown in Figure 2, cell viability was significantly decreased in a time- and dose-dependent manner in SiHa cell lines. After a 48 h incubation with 0, 2.5, 5, 10, 20, and 40 µM lochmolin F (**6**), cell survival decreased to 68.18%, 45.10%, 37.71%, 34.54%, and 36.27% in the SiHa cells compared to negative control. However, compound **6** showed no cytotoxicity against normal human cervical epithelial cells HUCEC at the concentration of 40 µM. Thus, the lochmolin F (**6**) might have the ability to inhibit SiHa cell proliferation selectively.

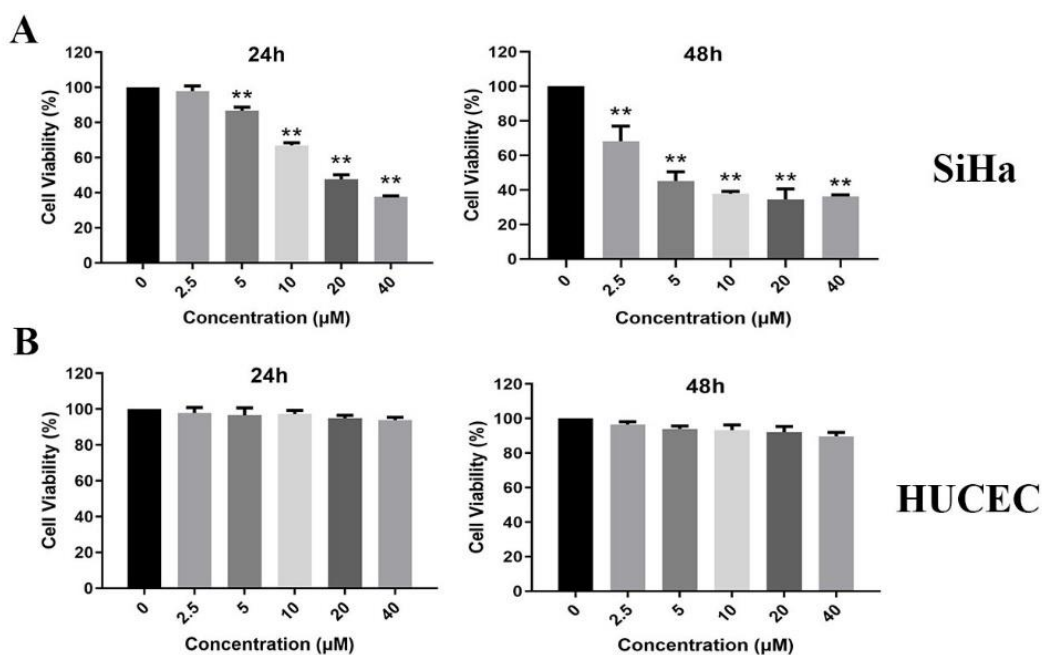


Figure 2. Lochmolin F (**6**) inhibited cell proliferation in SiHa and HUVEC cell lines after treatment with different concentrations (0, 2.5, 5, 10, 20, and 40 μM) of lochmolin F (**6**) for 24 h and 48 h. The data are presented as the mean \pm SD ($n = 3$) and were analyzed using one-way ANOVA followed by Tukey's post hoc test. * $P < 0.05$ and ** $P < 0.01$ versus the Control group.

3.5.2. Lochmolin F (**6**) Induced Apoptosis in SiHa Cell Lines

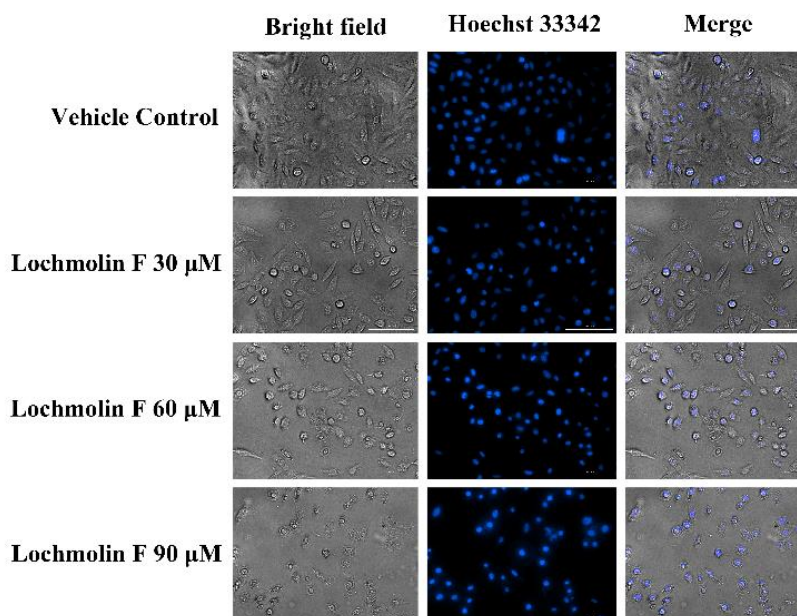


Figure 3. Cell morphology of SiHa cell lines was captured with a microscope after treatment with control (DMSO) or the indicated concentrations (30, 60, 90 μM) of lochmolin F (**6**) for 48 h. Scale bar, 100 μm .

Phytochemical composition isolated from *Aglaia perviridis*

To investigate the effect of lochmolin F (**6**) on the cell morphology of SiHa cell lines, cell lines treated with different concentrations (0, 30, 60, 90 μM) of lochmolin F (**6**) for 48 h were stained with the cell-permeable DNA dye Hoechst 33342. The nuclear morphological changes of cells were examined by fluorescent microscopy. As shown in Figure 3, the nucleus shrinks, and apoptotic bodies are formed. It was shown that the number of apoptotic bodies increased in a dose-dependent manner following the treatment of the cells with lochmolin F (**6**).

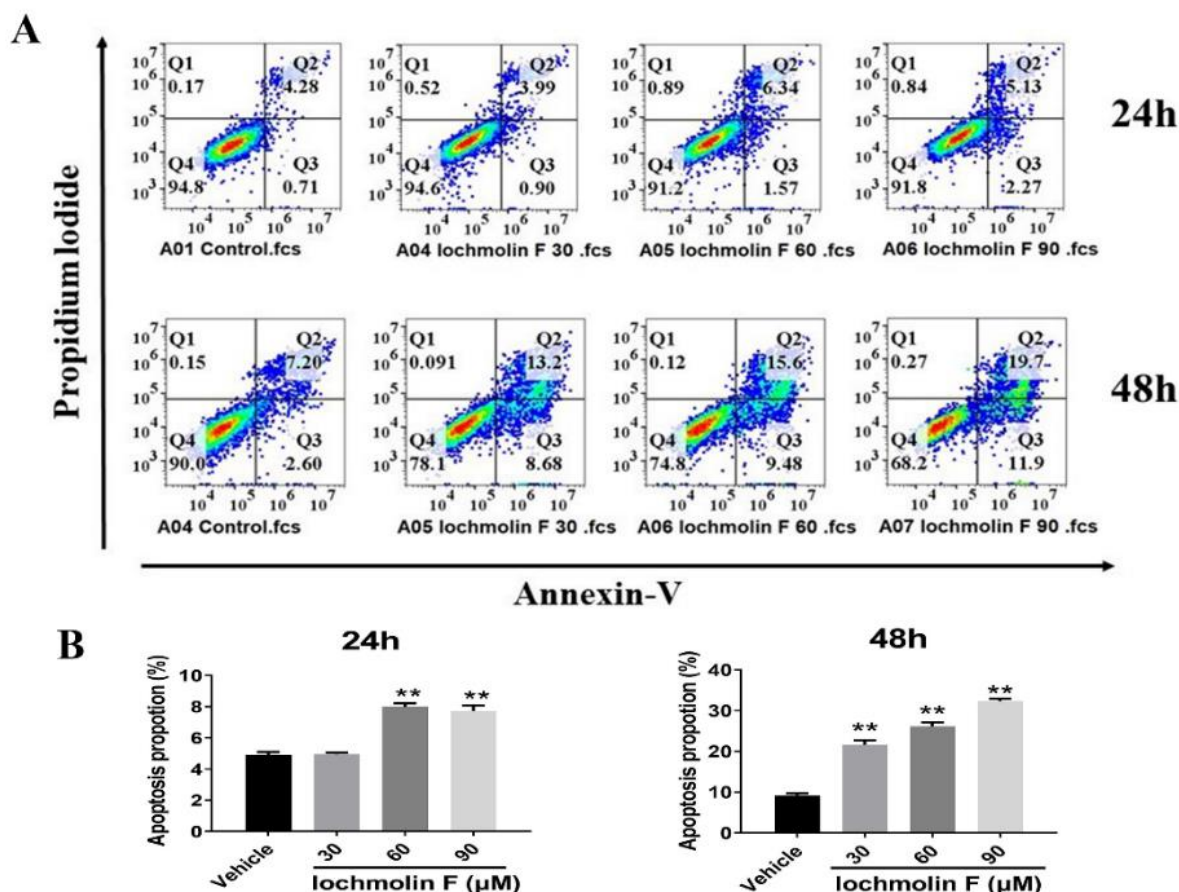


Figure 4. Lochmolin F (**6**) induced apoptosis in SiHa cell lines. (A) SiHa cell lines were treated with control (DMSO) or the indicated concentrations (30, 60, 90 μM) of lochmolin F (**6**) for 24 h and 48 h, followed by Flow cytometry analysis to determine the apoptosis proportion. (B) Late-stage apoptosis rate (Q2) and early-stage apoptosis (Q3) of cells were quantified. The data are presented as the mean \pm SD ($n=3$) and were analyzed using one-way ANOVA followed by Tukey's post hoc test. * $P<0.05$ and ** $P<0.01$ versus the Control group.

To further determine whether lochmolin F (**6**) induces SiHa cells apoptosis, cells treated with different concentrations (0, 30, 60, 90 μM) of lochmolin F (**6**) for 24 h and 48 h were double-stained with Annexin V/PI and then subjected to the flow cytometry. As shown in Figure 4A–B, the number of apoptotic cells in the treated SiHa cells increased in a time- and dose-dependent manner.

3.5.3. Lochmolin F (6) Induced S Cell Cycle Arrest in SiHa Cell Lines

To evaluate whether lochmolin F (6) could cause cell cycle arrest, we used flow cytometry analysis. The percentage of S phase cells in SiHa cultures was increased after treatment with different concentrations (0, 30, 60, 90 μM) of lochmolin F (6) for 24 h and 48 h (Figures 5A and 5B). We confirmed these results by detecting the expression levels of cyclin A2, cyclin D1, and CDK2 proteins, all of which are essential for the S phase [59]. After treatment with different concentrations (0, 30, 60, 90 μM) of lochmolin F (6) for 24 h, the expression levels of cyclin A2 and CDK2 proteins were decreased significantly (Figure 5C and 5D). Together, these data indicate that lochmolin F (6) induced SiHa cells to arrest at the S phase by inhibiting the expression levels of cyclin A2 and CDK2.

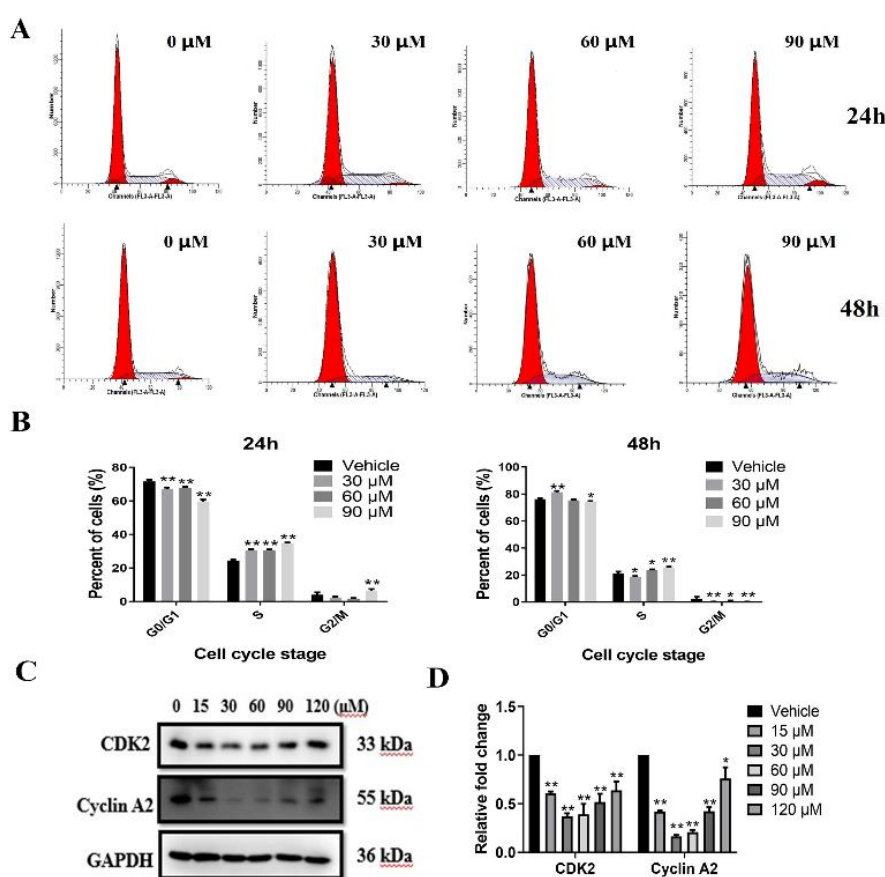


Figure 5. Lochmolin F (6) induced cell cycle arrest in SiHa cells. (A) SiHa cells were cultured with control (DMSO) or the indicated concentrations (30, 60, 90 μM) of lochmolin F (6) for 24 h and 48 h and analyzed by flow cytometry to assess the cell cycle arrest. (B) The number of SiHa cells in different cell cycle phases was quantified following flow cytometry. The data are presented as the mean \pm SD ($n=3$) and were analyzed using one-way ANOVA followed by Tukey's post hoc test. $*P<0.05$ and $**P<0.01$ versus the Control group. (C) Western blot was performed to analyze the expression changes of proteins CDK2 and Cyclin A2. The data are presented as the mean \pm SD ($n=3$) and were analyzed using one-way ANOVA followed by Tukey's post hoc test. $*P<0.05$ and $**P<0.01$ versus the Control group.

Acknowledgments

This work was financially supported by “Research Program of Changsha Central Hospital (grant no. YNKY202117), the Scientific Research Funds of Health Commission of Hunan Province (grant no. 202202042457), Hunan Provincial Department of Education funded research projects (22B0454) and the Science and Technology Program Foundation of Changsha (grant no. kq2202056)”.

Supporting Information

Supporting information accompanies this paper on <http://www.acgpubs.org/journal/records-of-natural-products>

ORCID

Donghua Cao: [0000-0003-2532-7854](https://orcid.org/0000-0003-2532-7854)

Binyuan Jiang: [0000-0002-4058-8377](https://orcid.org/0000-0002-4058-8377)

Linghui Cao: [0000-0002-9203-2477](https://orcid.org/0000-0002-9203-2477)

Manli Jiang: [0009-0005-8381-1849](https://orcid.org/0009-0005-8381-1849)

Xueting Liu: [0009-0002-5356-761X](https://orcid.org/0009-0002-5356-761X)

References

- [1] C. M. Pannell (1992). Taxonomic monograph of the genus *Aglaia* Lour. (Meliaceae). HMSO, London, England.
- [2] S. K. Chen, H. Li and P. Y. Cheng (1997). Chinese flora (Zhongguo Zhiwu Zhi). Science, Beijing, 43, pp. 69.
- [3] Ching Su New Medical College ed. (1997). Dictionary of Chinese crude drugs [in Chinese]. pp. 974.
- [4] L. Pan, J. L. Woodard, D. M. Lucas, J. R. Fuchs and A. D. Kinghorn (2014). Rocaglamide, silvestrol and structurally related bioactive compounds from *Aglaia* species, *Nat. Prod. Rep.* **31**, 924-39.
- [5] N. Ribeiro, F. Thuaud, C. Nebigil and L. Desaubry (2012). Recent advances in the biology and chemistry of the flavaglines, *Bioorg. Med. Chem.* **20**, 1857-64.
- [6] S. S. Ebada, N. Lajkiewicz, J. A. Porco, Jr., M. Li-Weber and P. Proksch (2011). Chemistry and biology of rocaglamides (= flavaglines) and related derivatives from *Aglaia* species (Meliaceae), *Prog. Chem. Org. Nat. Prod.* **94**, 1-58.
- [7] N. Joycharat, H. Greger, O. Hofer and E. Saifah (2008). Flavaglines and triterpenoids from the leaves of *Aglaia forbesii*, *Phytochemistry* **69**, 206-211.
- [8] Chaidir, W. H. Lin, R. Ebel, R. Edrada, V. Wray, M. Nimtz, W. Sumaryono and P. Proksch (2001). Rocaglamides, glycosides, and putrescine bisamides from *Aglaia dasyclada*, *J. Nat. Prod.* **64**, 1216-1220.
- [9] B. G. Wang, R. Ebel, C. Y. Wang, R. A. Edrada, V. Wray and P. Proksch (2004). Aglacins I-K, three highly methoxylated lignans from *Aglaia cordata*, *J. Nat. Prod.* **67**, 682-684.
- [10] D. Todt, N. Moeller, D. Praditya, V. Kinast, M. Friesland, M. Engelmann, L. Verhoye, I. M. Sayed, P. Behrendt, V. L. D. Thi, P. Meuleman and E. Steinmann (2018). The natural compound silvestrol inhibits hepatitis E virus (HEV) replication *in vitro* and *in vivo*, *Antivir. Res.* **157**, 151-158.

- [11] F. Elgner, C. Sabino, M. Basic, D. Ploen, A. Grunweller and E. Hildt (2018). Inhibition of Zika virus replication by silvestrol, *Viruses-Basel* **10**(4),149. doi: 10.3390/v10040149.
- [12] D. Engelmeier, F. Hadacek, T. Pacher, S. Vajrodaya and H. Greger (2000). Cyclopenta[b]benzofurans from *Aglaia* species with pronounced antifungal activity against rice blast fungus (*Pyricularia grisea*), *J. Agric. Food Chem.* **48**, 1400-1404.
- [13] B. Y. Hwang, B. N. Su, H. B. Chai, Q. W. Mi, L. B. S. Kardono, J. J. Afriastini, S. Riswan, B. D. Santarsiero, A. D. Mesecar, R. Wild, C. R. Fairchild, G. D. Vite, W. C. Rose, N. R. Farnsworth, G. A. Cordell, J. M. Pezzuto, S. M. Swanson and A. D. Kinghorn (2004). Silvestrol and episilvestrol, potential anticancer rocaglate derivatives from *Aglaia silvestris*, *J. Org. Chem.* **69**, 3350-3358.
- [14] F. L. An, X. B. Wang, H. Wang, Z. R. Li, M. H. Yang, J. Luo and L. Y. Kong (2016). Cytotoxic rocaglate derivatives from leaves of *Aglaia perviridis*, *Sci. Rep.* **6**, 20045. doi: 10.1038/srep20045.
- [15] L. Pan, U. M. Acuna, J. Li, N. Jena, N. Tran Ngoc, C. M. Pannell, H. Chai, J. R. Fuchs, E. J. C. de Blanco, D. D. Soejarto and A. D. Kinghorn (2013). Bioactive flavaglines and other constituents isolated from *Aglaia perviridis*, *J. Nat. Prod.* **76**, 394-404.
- [16] B. W. Nugroho, R. A. Edrada, V. Wray, L. Witte, G. Bringmann, M. Gehling and P. Proksch (1999). An insecticidal rocaglamide derivatives and related compounds from *Aglaia odorata* (Meliaceae), *Phytochemistry* **51**, 367-376.
- [17] H. Greger, T. Pacher, B. Brem, M. Bacher and O. Hofer (2001). Insecticidal flavaglines and other compounds from Fijian *Aglaia* species, *Phytochemistry* **57**, 57-64.
- [18] F. Zhang, Y. J. Chen, Y. Zhu, Q. Li and J. Cen (2016). A new triterpenoid from *Aglaia perviridis*, *Chem. Nat. Compd.* **52**, 427-431.
- [19] O. Yodsaoue, J. Sonprasit, C. Karalai, C. Ponglimanont, S. Tewtrakul and S. Chantrapromma (2012). Diterpenoids and triterpenoids with potential anti-inflammatory activity from the leaves of *Aglaia odorata*, *Phytochemistry* **76**, 83-91.
- [20] P. Sun, D. H. Cao, Y. D. Xiao, Z. Y. Zhang, J. N. Wang, X. C. Shi, C. F. Xiao, H. B. Hu and Y. K. Xu (2020). Aspidoptoids A-D: Four new diterpenoids from *Aspidopterys obcordata* Vine, *Molecules* **25**, 529; doi:10.3390/molecules25030529.
- [21] S. Wei, M. Xiong, Z. Da-Qian, L. Bin-Yong, W. Yang-Yang, D. H. Gutmann, H. Zhi-Yong and C. Xiao-Ping (2012). Ku80 functions as a tumor suppressor in hepatocellular carcinoma by inducing S-phase arrest through a p53-dependent pathway, *Carcinogenesis*, **33**, 538-547.
- [22] J. Li, M. Liu, Y. Li, D. D. Sun, Z. Shu, Q. Tan, S. Guo, R. Xie, L. Gao, H. Ru, Y. Zang, H. Liu, J. Li and Y. Zhou (2020). Discovery and optimization of non-bile acid FXR agonists as preclinical candidates for the treatment of nonalcoholic steatohepatitis, *J. Med. Chem.* **63**, 12748-12772.
- [23] E. Saifah, J. Puripattavong, K. Likhitwitayawuid, G. A. Cordell, H. Chai and J. M. Pezzuto (1993). Bisamides from *Aglaia* species: structure analysis and potential to reverse drug resistance with cultured cells, *J. Nat. Prod.* **56**, 473-477.
- [24] Y. W. Chin, H. S. Chae, J. Lee, T. B. Tran, K. S. Ahn, H. K. Lee, H. Joung and S. R. Oh (2010). Bisamides from the twigs of *Aglaia perviridis* collected in Vietnam, *B. Korean Chem. Soc.* **31**, 2665-2667.
- [25] Y. J. Tseng, K. P. Shen, H. L. Lin, C. Y. Huang, C. F. Dai and J. H. Sheu (2012). Lochmolins A-G, New Sesquiterpenoids from the Soft Coral *Sinularia lochmodes*, *Mar. Drugs* **10**, 1572-1581.

Phytochemical composition isolated from *Aglaia perviridis*

- [26] Q. J. Ma, L. Han, X. X. Bi, X. B. Wang, Y. Mu, P. P. Guan, L. Y. Li and X. S. Huang (2016). Structures and biological activities of the triterpenoids and sesquiterpenoids from *Alisma orientale*, *Phytochemistry* **131**, 150-157.
- [27] Y. H. Kuo, C. H. Chen, S. C. Chien and Y. L. Lin (2002). Five new cadinane-type sesquiterpenes from the heartwood of *Chamaecyparis obtusa* var. *formosana*, *J. Nat. Prod.* **65**, 25-28.
- [28] B. N. Su, H. Y. Chai, Q. W. Mi, S. Riswan, L. B. S. Kardono, J. J. Afriastini, B. D. Santarsiero, A. D. Mesecar, N. R. Farnsworth, G. A. Cordell, S. M. Swanson and A. D. Kinghorn (2006). Activity-guided isolation of cytotoxic constituents from the bark of *Aglaia crassinervia* collected in Indonesia, *Bioorg. Med. Chem.* **14**, 960-972.
- [29] N. Nakamura, S. Kojima, Y. A. Lim, M. R. Meselhy, M. Hattori, M. P. Gupta and M. Correa (1997). Dammarane-type triterpenes from *Cordia spinescens*, *Phytochemistry* **46**, 1139-1141.
- [30] H. Itokawa, E. Kishi, H. Morita and K. Takeya (1992). Cytotoxic quassinoids and tirucallane-type triterpenes from the woods of *Eurycoma longifolia*, *Chem. Pharm. Bull.* **40**, 1053-1055.
- [31] M. Arisawa, A. Fujita, N. Morita, P. J. Cox, R. A. Howie and G. A. Cordell (1987). Triterpenes from *Simaba multiflora*, *Phytochemistry* **26**, 3301-3303.
- [32] W. Wang, Z. R. Xu, M. Yang, R. X. Liu, W. X. Wang, P. Liu and D. Guo (2007). Structural determination of seven new triterpenoids from *Kadsura heteroclita* by NMR techniques, *Magn. Reson. Chem.* **45**, 522-526.
- [33] A. Inada, H. Murata, Y. Inatomi, T. Nakanishi and D. Darnaedi (1997). Pregnanes and triterpenoid hydroperoxides from the leaves of *Aglaia grandis*, *Phytochemistry* **45**, 1225-1228.
- [34] K. K. Purushothaman, A. Sarada and A. Saraswathy (1987). Chemical constituents of *Lansium anamallayanum* bedd., *Can. J. Chem.* **65**, 150-153.
- [35] Q. Y. Zhang, G. Wu, S. Y. Liu, Y. Y. Zhao and T. M. Cheng (2002). New steroid glycoside derivatives from *Stelmatocrypton khasianum*, *Chin. Tradit. Herb. Drugs* **1**, 8-10.
- [36] J. Latip, T. G. Hartley and P. G. Waterman (1999). Lignans and coumarins metabolites from *Melicope hayesii*, *Phytochemistry* **51**, 107-110.
- [37] W. J. Zhang, Y. Wang, Z. F. Geng, S. S. Guo, J. Q. Cao, Z. Zhang, X. Pang, Z. Y. Chen, S. S. Du and Z. W. Deng (2018). Antifeedant activities of lignans from stem bark of *Zanthoxylum armatum* DC. against *Tribolium castaneum*, *Molecules* **23**(3), 617. doi: 10.3390/molecules23030617.
- [38] Y. Ge, Y. Z. Wang, P. P. Chen, Y. F. Wang, C. C. Hou, Y. B. Wu, M. L. Zhang, L. G. Li, C. H. Huo, Q. W. Shi and H. X. Gao (2016). Polyhydroxytriterpenoids and phenolic constituents from *Forsythia suspensa* (Thunb.) Vahl leaves, *J. Agric. Food Chem.* **64**, 125-131.
- [39] Y. Zhao, L. Z. Liang, H. J. Li, S. Y. Wen and E. J. Lan (2012). Chemical constituents of *Clematis chinensis* Osbeck, *Acta Sci. Nat. Univ. Sunyatseni* **51**, 63-67.
- [40] V. Seidel, F. Bailleul and P. G. Waterman (2000). (Rel)-1 β ,2 α -di-(2,4-dihydroxy-6-methoxybenzoyl)-3 β , 4 α -di-(4-methoxyphenyl)-cyclobutane and other flavonoids from the aerial parts of *Goniothalamus gardneri* and *Goniothalamus thwaitesii*, *Phytochemistry* **55**, 439-446.
- [41] X. M. Li, J. M. Liu, Y. Zhang and B. G. Wang (2007). Chemical constituents from *Aglaia odorata* Lour, *Chin. Tradit. Herb. Drugs* **3**, 356-357.
- [42] H. Dong, Y. L. Gou, S. G. Cao, S. X. Chen, K. Y. Sim, S. H. Goh and R. M. Kini (1999). Eicosenones and methylated flavonols from *Amomum koenigii*, *Phytochemistry* **50**, 899-902.
- [43] G. Q. Liu, H. Tatematsu, M. Kurokawa, M. Niwa and Y. Hirata (1984). Novel C-3-C-3"-biflavanones from *Stellera chamaejasme*, *Chem. Pharm. Bull.* **32**, 362-365.

- [44] Y. Li, B. D. Sun, S. C. Liu, L. H. Jiang, X. Z. Liu, H. Zhang and Y. S. Che (2008). Bioactive asteric acid derivatives from the Antarctic Ascomycete fungus *Geomyces* sp, *J. Nat. Prod.* **71**, 1643-1646.
- [45] A. EstevezBraun, R. EstevezReyes and A. G. Gonzalez (1996). C-13 NMR assignments of some dibenzyl-gamma-butyrolactone lignans, *Phytochemistry* **43**, 885-886.
- [46] D. H. Cao, S. G. Liao, P. Sun, Y. D. Xiao and Y. K. Xu (2020). Mexicanolide-type limonoids from the twigs and leaves of *Cipadessa baccifera*, *Phytochemistry* **177**, 112449.
- [47] Y. K. Zheng, Y. Q. Wang, B. J. Su, H. S. Wang, H. B. Liao and D. Liang (2022). New enantiomeric lignans and new meroterpenoids with nitric oxide release inhibitory activity from *Piper puberulum*, *Bioorg. Chem.* **119**, 05522. doi: 10.1016/j.bioorg.2021.105522
- [48] H. Zhang, H. H. Xu, Z. J. Song, L. Y. Chen and H. J. Wen (2012). Molluscicidal activity of *Aglaia duperreana* and the constituents of its twigs and leaves, *Fitoterapia* **83**, 1081-1086.
- [49] Y. S. Y. Yeap, N. K. Kassim, R. C. Ng, G. C. L. Ee, L. S. Yazan and K. H. Musa (2017). Antioxidant properties of ginger (*Kaempferia angustifolia* Rosc.) and its chemical markers, *Int. J. Food Propert.* **20**, S1158-S1172.
- [50] P. K. Mishra, B. K. Sarma, P. K. Singhai and U. P. Singh (2007). Antifungal activity of 2-hydroxy 4,4'6'tri-methoxy chalcone, *Mycobiology* **35**, 72-75.
- [51] Jasril, L. Y. Mooi, N. H. Lajis, A. M. Ali, M. A. Sukari, A. A. Rahman, A. G. Othman, H. Kikuzaki and N. Nakatani (2003). Antioxidant and antitumor promoting activities of the flavonoids from *Hedychium thyriforme*, *Pharm. Biol.* **41**, 506-511.
- [52] C. Yan, Y. D. Zhang, X. H. Wang, S. D. Geng, T. Y. Wang, M. Sun, W. Liang, W. Q. Zhang, X. D. Zhang and H. Luo (2016). Tirucallane-type triterpenoids from the fruits of *Phellodendron chinense* Schneid and their cytotoxic activities, *Fitoterapia* **113**, 132-138.
- [53] Z. L. Hong, J. Xiong, S. B. Wu, J. J. Zhu, J. L. Hong, Y. Zhao, G. Xia and J. F. Hu (2013). Tetracyclic triterpenoids and terpenylated coumarins from the bark of *Ailanthus altissima* ("Tree of Heaven"), *Phytochemistry* **86**, 159-167.
- [54] S. I. Kurimoto, Y. Kashiwada, K. H. Lee and Y. Takaishi (2011). Triterpenes and a triterpene glucoside from *Dysoxylum cumingianum*, *Phytochemistry* **72**, 2205-2211.
- [55] X. N. Wang, C. Q. Fan, S. Yin, L. P. Lin, J. Ding and J. M. Yue (2008). Cytotoxic terpenoids from *Turraea pubescens*, *Helv. Chim. Acta* **91**, 510-519.
- [56] S. L. Wu, Q. P. Zou, X. Y. Xie, J. J. Ren, Z. Fan, J. R. OuYang, P. C. Yin, F. W. Dong and H. P. He (2022). Two new triterpenoids from the fruits of *Aphanamixis polystachya*, *J. Asian Nat. Prod. Res.* **24**, 738-745.
- [57] C. L. Bowlus (2016). Obeticholic acid for the treatment of primary biliary cholangitis in adult patients: clinical utility and patient selection, *Hepatic Med-Evid. Res.* **8**, 89.
- [58] D. Chianelli, P. V. Rucker, J. Roland, D. C. Tully, J. Nelson, X. Liu, B. Bursulaya, E. D. Hernandez, J. Wu and M. Prashad (2020). Nidufexor (LMB763), a novel FXR modulator for the treatment of nonalcoholic steatohepatitis, *J. Med. Chem.* **63**, 3868-3880.
- [59] R. A. Woo and R. Poon (2003). Cyclin-dependent kinases and S phase control in mammalian cells, *Cell Cycle* **2**, 315-323.